Optica Applicata, Vol. XVII, No. 1, 1987

Variable wavelength interferometry. V. Application to birefringent objects

MAKSYMILIAN PLUTA

Central Optical Laboratory, ul. Kamionkowska 18, 03–805 Warszawa, Poland

Four papers presented earlier dealt with the variable wavelength interferometry (VAWI) of isotropic objects. Now, the original transmitted-light VAWI method and its modifications, the VAWI–2 and VAWI–3 techniques, are offered for the study of anisotropic objects such as birefringent textile fibres, double-refracting phase retarders, birefringent foils, and other like objects.

1. Introduction

Variable wavelength interferometry (VAWI) presented in a series of papers [1–4] can also be applied to the study of birefringent objects. This method is especially useful for measuring birefringence of textile fibres and for testing birefringent retarders. Its advantages appear to be obvious when it is used together with a double-refracting interferometer such as the Biolar PI microinterferometer. Consequently, this instrument will be taken into consideration in this part of the work.

The versions of the transmitted-light VAWI method will be discussed here: 1) the VAWI–1 technique, which is identical with the original VAWI method, 2) the VAWI–2 and 3) the VAWI–3 techniques. The first two techniques were already discussed in Parts 1 and 3 of this work [1], [3], and now they will be adapted to birefringent objects, while the VAWI–3 technique is the alternative of the VAWI–2 technique when optical path differences produced by birefringent objects are relatively large.

The original VAWI method [1] requires interference patterns which contain simultaneously interference fringes displaced by an object under study and reference (undisplaced) fringes; both fringes are brought into their mutually coincident or anticoincident positions when the wavelength of monochromatic light is continuously varied. The method applies therefore to birefringent fibres and the like objects. In practice, however, there are double-refracting objects which do not permit us to observe simultaneously the displaced and reference fringes. Among such objects there are birefringent foils, birefringent phase retarders (λ-, $\lambda/2$- or $\lambda/4$-plates), and other objects; they cannot effectively be measured using the original VAWI method (or VAWI–1 technique). Fortunately, this limitation does not exist if the VAWI–2 or VAWI–3 technique is used.

In contrast to the original VAWI method, the VAWI–2 technique [4] is based

on another form of interference fringe coincidence. For this operation, a gauging graticule consisting of two pointer lines is used. The zero-order fringe of the empty interference field is adjusted to achieve the coincidence with one pointer line and the displaced fringes of high orders are consecutively brought into coincidences with the other pointer line when the wavelength of monochromatic light is continuously varied within a large region of the visible spectrum. The distance (d) between the pointer lines is selected as long as possible if the optical path difference to be measured is small. On the other hand, if birefringent objects produce relatively significant optical path differences, say greater than 3λ, the distance d should be small or even equal to zero. In the latter instance, a single pointer line is used, and the interferometric procedure is referred to as the VAWI–3 technique.

2. VAWI–1 technique

Let a birefringent fibre or the like object be placed on the stage of the Biolar PI microinterferometer. The objective Wollaston prism W_o of this instrument is adjusted subtractively with respect to the tube Wollaston prism W_2 (Fig. 1). The fibre is transparent in visible spectrum and its directional refractive indices $n_{\parallel}$ and $n_{\perp}$ are characterized by typical dispersion curves $n_{\parallel}(\lambda)$ and $n_{\perp}(\lambda)$. It is also assumed that $n_{\parallel}$ and $n_{\perp}$ are constant across the fibre diameter and that a parallel beam of monochromatic light with continuously variable wavelength strikes the fibre

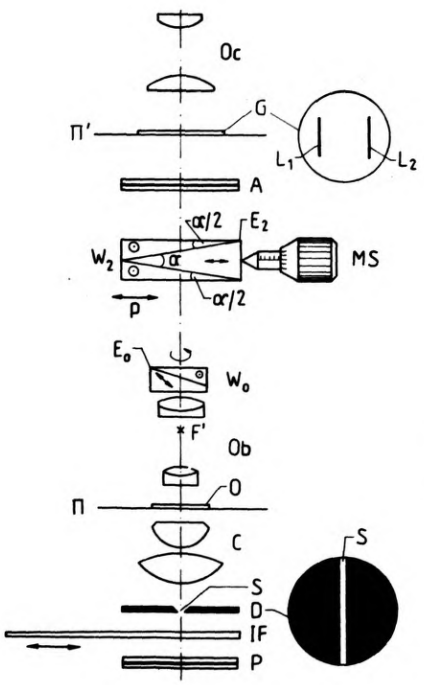

Fig. 1. Optical system of a double-refracting interference system (Biolar PI microinterferometer). P – polarizer, IF – wedge interference filter, D – slit diaphragm, S – slit, C – condenser, Π – object plane, O – object under study, Ob – low-power microscope objective, W_o and W_2 – double-refracting prisms (modified Wollaston prisms made of quartz crystal), MS – micrometer screw, A – analyser, Π' – image plane, G – graticule with two pointer lines L_1 and L_2, Oc – ocular

normally. In order to measure the fibre birefringence, the basic elements of the Biolar PI microinterferometer are oriented as shown in Fig. 2**a**. As can be seen, the polarizer P and analyser A are crossed and their direction of light vibration (PP and AA) form an angle of 45° with the apex edge (E_2) of the Wollaston prism W_2. A birefringent fibre under study (F) is oriented diagonally with respect to the directions of light vibration in the polarizer and analyser.

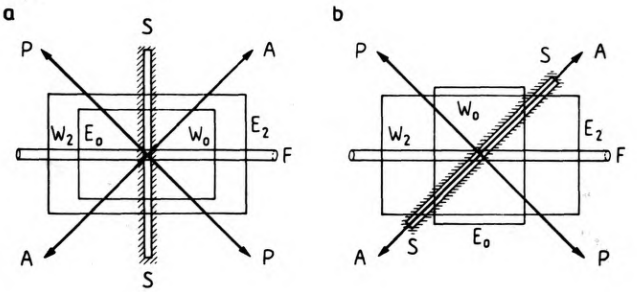

Fig. 2. Basic orientations of principal elements of the Biolar PI instrument (Fig. 1) used for microinterferometric study of birefringent fibres and other like objects. **a** – objective birefringent prism W_o is adjusted subtractively with respect to the tube birefringent prism W_2; measurement of fibre birefringence, **b** – birefringent prism W_o is crossed with W_2; measurement of fibre refractive indices $n_{\|}$ and $n_{\perp}$. PP and AA – directions of light vibration in the polarizer and analyser, respectively; SS – direction of the condenser slit; E_0 and E_2 – apex edges of the double-refracting prisms W_o and W_2, respectively; F – birefringent fibre (oriented diagonally with respect to PP and AA)

Given these assumptions, an optical path difference δ arises between light wave components whose vibrations are parallel (||) and perpendicular ($\perp$) to the fibre axis. This quantity is defined as

$$\delta = (n_{\|} - n_{\perp})t = Bt \tag{1}$$

where $B = n_{\|} - n_{\perp}$ is the fibre birefringence and t is the fibre thickness in a direction parallel to the optical axis of the microinterferometer objective Ob (Fig. 1).

The optical path difference δ causes the interference fringes I′ (Fig. 3) to be displaced along the fibre image observed in the image plane Π' (Fig. 1) of the Biolar PI microinterferomenter. If the wavelength λ of the incident light is continuously decreased or increased by means a wedge interference filter (IF, Fig. 1), then the interference fringes move towards or away from the low-order fringes; thus the interfringe spacing (b) varies with wavelength λ of monochromatic light. Consequently, starting from a long wavelength it is possible to select such a particular wavelength λ_1 (Fig. 3**a**) for which the peaks of interference fringes (I′) displaced by the fibre under study occupy the positions coincident with the location of the reference (undisplaced) fringes (I). Such a coincidence is always possible if the optical path difference δ is not too small (say, $\delta > \lambda$) and can be

expressed as

$$\delta_1 = (n_{\parallel 1} - n_{\perp 1})\, t = B_1\, t = m_1\, \lambda_1 \tag{2}$$

where m_1 is an integer number referred to as the initial interference order. However, if the fibre introduces a significant optical path difference δ (several times greater than λ), then the further fringe coincidences occur if λ decreases (Fig. 3**c**). Each two consecutive coincidences are separated by a fringe anticoincidence (Fig. 3**b**). All these coincidences and anticoincidences can be expressed by a family

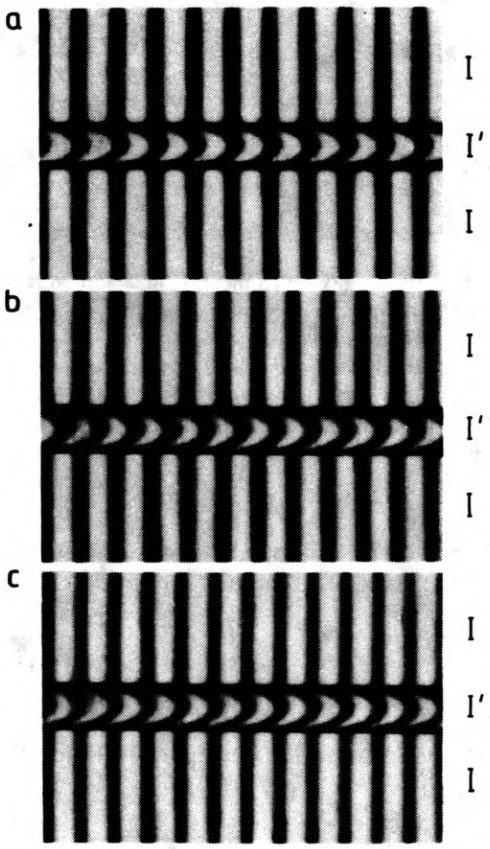

Fig. 3. Principle of the VAWI–1 technique used for the measurement of fibre birefringence

of equations similar to Eq. (2). For the sake of brevity, this equation family may be expressed as

$$\delta_s = (n_{\parallel s} - n_{\perp s})\, t = B_s\, t = (m_1 + q_s)\, \lambda_s \tag{3}$$

where $s = 2, 3, 4, \ldots$ and $q_s = 0.5, 1, 1.5, \ldots$. The parameter q_s is referred to as the increment of the current interference order m with respect to the initial interference order m_1 when the light wavelength λ decreases from λ_1 to λ_2, λ_3, λ_4, ... Consequently, $m = m_1 + q_s$.

From Eqs. (2) and (3) it follows that

$$m_1 = q_s \frac{\lambda_s}{B_{s1}\lambda_1 - \lambda_s} \tag{4}$$

where

$$B_{s1} = \frac{B_s}{B_1} = \frac{n_{\parallel s} - n_{\perp s}}{n_{\parallel 1} - n_{\perp 1}}. \tag{5}$$

As mentioned earlier, the interfringe spacing b varies with wavelength λ of monochromatic light; this variation is mathematically described by a quite simple relation

$$b = \lambda/\varepsilon, \tag{6}$$

where ε is given by

$$\varepsilon = D\tan\alpha. \tag{7}$$

Here α is the apex angle of the tube Wollaston prism W_2 (Fig. 1) and D is its double-refracting power. For a typical Wollaston prism,

$$D = 2(n_e - n_o) \tag{8}$$

where n_e and n_o are the extraordinary and ordinary refractive indices of a double-refracting material of which the prism is made.

From Eq. (6) it follows that the wavelengths λ_1 and λ_s occurring in Eq. (4) may be expressed as

$$\lambda_1 = b_1\varepsilon_1 \quad \text{and} \quad \lambda_s = b_s\varepsilon_s. \tag{9}$$

Hence, Eq. (4) may be rewritten as

$$m_1 = q_s \frac{b_s}{B_{s1}D_{1s}b_1 - b_s} \tag{10}$$

where

$$D_{1s} = \frac{\varepsilon_1}{\varepsilon_s} = \frac{D_1}{D_s} = \frac{n_{e1} - n_{o1}}{n_{es} - n_{os}}. \tag{11}$$

The coefficients B_{s1} and D_{1s} express the spectral dispersion of birefringance; however, B_{s1} refers to the object under study, while D_{1s} applies to the Wollaston prism W_2 of the double-refracting microinterferometer (Fig. 1). It is possible that dispersion curves $B(\lambda)$ and $D(\lambda)$ are similar to each other; in this case $B_{s1}D_{1s} = 1$ and Eq. (10) takes a quite simple form

$$m_1 = q_s \frac{b_s}{b_1 - b_s}. \tag{12}$$

An interferometric situation which satisfies the above equation will be called the

object adapted interferometry (OAI). This kind of interferometry offers new measuring possibilities; they are discussed in more detail in a separate paper [5].

Equation (12) expresses a very important relation for the VAWI techniques. Namely, it has experimentally been stated that this equation may generally be used for calculating the initial interference order m_1 when the spectral dispersion of birefringence $B(\lambda)$ of objects to be studied differs from that $D(\lambda)$ of the Wollaston prism made of quartz crystal. For many birefringent materials, the term $B_{s1} D_{1s}$ is nearly equal to unity and Eq. (12) is generally a good approximation to the exact formula (10). In order to illustrate this statement, the values of the term $B_{s1} D_{1s}$ for the spectral lines F and C and for a few birefringent fibres are given in Table 1. As can be seen, $B_{FC} D_{CF}$ is only slightly greater than unity. Thus,

Table 1. Values of the term $B_{FC} D_{CF}$ for some birefringent fibres (according to data given in [6] and [7] and for the Wollaston prism made of quartz crystal whose $D_F = 0.00930$, $D_C = 0.00903$, $D_F - D_C = 0.00027$, $D_{CF} = 0.9710$

Material and fibre thickness t	B_F	B_C	$B_F - B_C$	B_{FC}	$B_{FC} D_{CF}$
PA6, $t = 28$ μm	0.0575	0.0555	0.0020	1.036	1.006
PET, $t = 22$ μm	0.178	0.165	0.013	1.079	1.048
PET, $t = 26$ μm	0.141	0.127	0.014	1.110	1.078
Poly(p-phenylene terephtalamide), $t = 13.6$ μm	0.780	0.700	0.08	1.114	1.082

putting $B_{s1} D_{1s} = 1$ in Eq. (10) yields, for the initial interference order m_1, a number only slightly higher than the expected integral number. If, for instance, it follows $m_1 = 9.3$ from Eq. (12), then the initial interference order m_1 is in fact equal to 9.

The main goal of the above described procedure is to determine the birefringence $n_{\parallel} - n_{\perp} = B$ of the object under study. We can distinguish two basic steps that lead to this goal. The first one it to measure the interfringe spacings $b_1, b_2, b_3, \ldots$ for consecutive fringe coincidences and anticoincidences to which the current interference orders $m = m_1, m_1 + 0.5, m_1 + 1, m_1 + 1.5, \ldots$ correspond, then calculate the initial interference order m_1 from Eq. (12), read out the wavelengths $\lambda_1, \lambda_2, \lambda_3, \ldots$ from the calibration graph $b(\lambda)$, calculate the optical path differences $\delta_1 = m_1 \lambda_1$, $\delta_2 = (m_1 + 0.5)\lambda_2$, $\delta_3 = (m_1 + 1)\lambda_3, \ldots$ and plot the graph $\delta(\lambda)$. The calibration graph $b(\lambda)$ must be carried out very carefully using highly monochromatic light, e.g., emitted by He-Ne-, Ar-, and He-Cd-lasers, whose light wavelengths are known very accurately; once plotted graph $b(\lambda)$ is valid premanently for a given instrument Biolar PI [8]. The second step is to determine the birefringences $B_1 = \delta_1/t$, $B_2 = \delta_2/t$, $B_3 = \delta_3/t, \ldots$ and plot the graph $B(\lambda)$ from which we can read out B for an arbitrary wavelength within the spectrum of light used. If the fibre or other object under study is cylindrical, its thikness t can be determined by measuring the fibre diameter. Otherwise, t must be determined in another way.

Sometimes it is also useful to take the interference order increment $q = -0.5$ for $\lambda > \lambda_1$ (in this case q is a decrement rather than increment). Frequently, the increments $q_s = 0.5, 1.5, 2.5, \ldots$ can be ignored since $q_s = 0, 1, 2, \ldots$ are quite sufficient for obtaining final results of interest. In general, the fringe coincidences (Figs. 3**a** and **c**), to which $q_s = 0, 1, 2, \ldots$ correspond, are adjusted more precisely than fringe anticoincidences (Fig. 3**b**), to which $q_s = 0.5, 1.5, 2.5, \ldots$ correspond. Especially, this holds good when the estimation of the fringe coincidences and/or anticoincidences is performed visually.

The birefringence $B = n_{\parallel} - n_{\perp}$ can also be determined by using a VAWI procedure that leads to determination of the refractive indices $n_{\parallel}$ and $n_{\perp}$ separately. The procedure is the same as for isotropic objects; it was described earlier [1], [3], and here it is only worth while mentioning that this procedure requires the crossed orientation of the objective Wollaston prism W_o (Fig. 1) with respect to the tube prism W_2 as shown in Fig. 2**b**. The interference image of a fibre of fibre-like object is now split into two images, one of which "contains" the refractive index $n_{\parallel}$ and the other the refractive index $n_{\perp}$.

3. VAWI–2 technique

The VAWI–1 technique described in Section 2 is suitable for the study of birefringent objects which produce relatively large optical path differences δ, say, greater than 3λ. For δ smaller than 3λ, this technique does not permit us to obtain a sufficient number of interference fringe coincidences and/or anticoincidences within the visible spectrum. This drawback is removed by the VAWI–2 technique. It uses a gauging graticule consisted of two pointer lines L_1 and L_2 (Fig. 4). The zero-order fringe I_0 of the empty (reference) interference field is adjusted to achieve its coincidence with one pointer line L_1, and the high-order fringes I′ displaced by the object under study are consecutively led to coincidences with the other pointer line L_2, when the wavelength of monochromatic light is continuously varied within the visible spectrum. The distance d between the pointer lines should be fixed as long as possible, say, $d = 10b$ if the optical path differences to be determined are small.

This procedure has been described earlier for isotropic objects [4] and the previous description holds good in the case of studying birefringent fibres and the like objects. The initial interference order m_1 is now expressed by the following formula:

$$m_1 = q_s \frac{b_s}{B_{s1} D_{1s} b_1 - b_s} + d \frac{B_{s1} D_{1s} - 1}{B_{s1} D_{1s} b_1 - b_s}. \tag{13}$$

If, however, the term $B_{s1} D_{1s}$ may be assumed to be equal to unity, the formula (12) holds also good for the VAWI–2 technique. In this case, the preferable interference order increments q_s are also equal to 0, 0.5, 1, 1.5, 2, ... These increments are not measured but fixed visually when consecutive dark (Fig. 4**a**) and

bright (Fig. 4**b**) interference fringes I′ are brought into coincidence with the pointer line L_2. For the first (initial) coincidence of a high-order dark fringe I′ (Fig. 4**a**), the increment $q_s = q_1 = 0$, current interference order m is equal to the initial interference order m_1, interfringe spacing $b = b_1$, and wavelength $\lambda = \lambda_1$. Then, for $\lambda_2 < \lambda_1$ the first coincidence of the adjacent bright fringe appears (Fig. 4**b**), and $q_s = q_2 = 0.5$, $m = m_1 + 0.5$, $b = b_2 < b_1$. The next dark fringe coincides with the pointer line L_2 for $\lambda_3 < \lambda_2$: now $q_s = q_3 = 1$, $m = m_1 + 1$, and $b = b_3 < b_2$. The next bright fringe coincides with L_2 for $q_s = q_4 = 1.5$, $m = m_1 + 1.5$, $b = b_4 < b_3$, and $\lambda = \lambda_4 < \lambda_3$, etc. As previously (see Sect. 2), the interfringe spacings b_1, b_2, b_3, ... are only measured. In contrast to these parameters, the increments q_1, q_2, q_3, ... are observed, while the wavelengths λ_1, λ_2, λ_3, ... are read out from the calibration plot $b(\lambda)$.

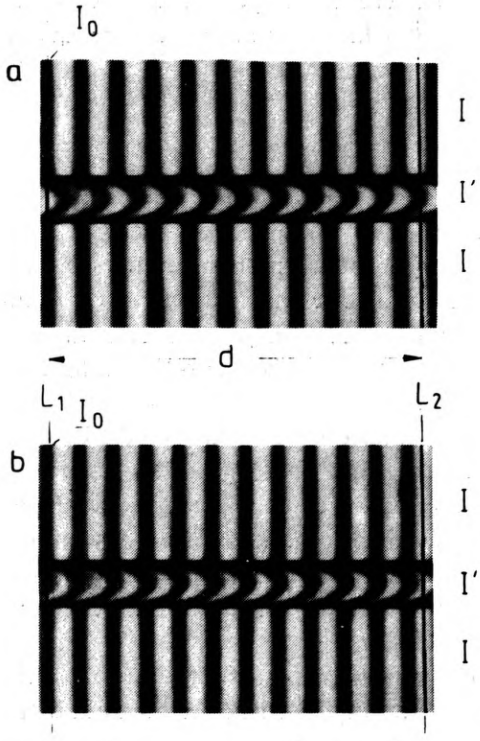

Fig. 4. Principle of the VAWI-2 technique used for the measurement of fibre birefringence

In order to determine the fibre birefringence $B = n_{\parallel} - n_{\perp}$, two graphs $b(m)$ or $\lambda(m)$ are plotted. One of these graphs refers to the empty interference field (see [4], for details) and the other to the interference image of the fibre under study. Additionally, optical path differences Δ_1, Δ_2, Δ_3, ... for the empty interference field and those Δ'_1, Δ'_2, Δ'_3, ... for the fibre image can be calculated from the relation $\Delta = m\lambda$, and the graphs $\Delta(\lambda)$ and $\Delta'(\lambda)$ are plotted. The optical path difference δ produced by the fibre birefringence is derived from the relation

$$\delta = (m_f - m_r)\lambda = \Delta' - \Delta \tag{14}$$

where $m_f - m_r$ is the difference in the current interference orders read out from the graphs $b(m)$ or $\lambda(m)$ mentioned above. Similarly, the difference $\Delta' - \Delta$ can be read out from the respective graphs $\Delta(\lambda)$ and $\Delta'(\lambda)$.

The directional refractive indices $n_{\parallel}$ and $n_{\perp}$ are separately determined in a way similar to that described earlier [4] for isotropic objects. The principal elements of the Biolar PI microinterferometer are of course adjusted as shown in Fig. 2**b**.

An important advantage of the VAWI–2 technique is a self-evident fact that we need not observe simultaneously the interference fringes I′ (Fig. 4) displaced by an object under study and the reference (undisplaced) fringes I. Consequently, phase plates (λ-, $\lambda/2$-, $\lambda/4$-retarders made of a birefringent material), birefringent foils, and other extended plate-like doublerefracting elements may easily be tested using this technique. In order to determine the phase retardation $\varphi = 2\pi\delta/\lambda$ of the objects mentioned above, the reference plot $b(m)$ or $\lambda(m)$ and the graph $\Delta(\lambda)$ which characterize the empty interference field may be ignored. Instead, the object under study is adjusted at two azimuths: $\Theta = +45°$ and $\Theta = -45°$, and two graphs $b'(m')$ and $b''(m'')$ or $\Delta'(\lambda)$ and $\Delta''(\lambda)$ are plotted (here Θ is the angle between the fast (or slow) axis of a birefringent object and the direction PP of light vibration in the polarizer P of a double-refracting interferometer – see Figs. 1 and 2). The optical path difference δ is then derived from the relation

$$2\delta = (m'' - m')\lambda = \Delta'' - \Delta' \tag{14}$$

where $m'' - m'$ is the difference in the current interference orders read out from the graphs $b'(m')$ and $b''(m'')$ for a given light wavelength λ. Similarly, the difference $\Delta'' - \Delta'$ can be read out from the respective graphs $\Delta'(\lambda)$ and $\Delta''(\lambda)$. In practice, the relative phase retardation $\varrho = \delta/\lambda$ is frequently in use. This quantity is simply given by

$$\varrho = \frac{m'' - m'}{2} = \frac{\Delta'' - \Delta'}{2\lambda}. \tag{15}$$

Like the VAWI 1 technique the VAWI–2 procedure is based on measuring directly only one parameter, i.e., the interfringe spacings $b_1, b_2, b_3, \ldots$. The measurement is performed with the help of a micrometer screw (MS, Fig. 1) precisely associated with the transverse movement of the Wollaston prism W_2. This movement is accompanied with an equivalent movement of the interference fringes observed in the image plane π', and the fringe centres are precisely guided onto one of the pointer lines. The measurement of multiple interfringe spacings, for instance, the distance between interference fringes of plus and minus twenty orders, rather than a single interfringe interval is recomended, leading to extremely accurate values for the spacings $b_1, b_2, b_3, \ldots$. However, it is important to note that the Wollaston prism W_2 must be carefully readjusted to its zero position determined by the coincidence of the pointer line L_1 (Fig. 4) with the zero-order fringe I_0 of the empty interference field, when one of the particular interfringe spacings has been measured. This zero position may readily be found by readjusting the micrometer screw MS (Fig. 1) to its originally fixed position, when the fringe I_0 was guided onto the pointer line L_1 for the first time.

4. VAWI–3 technique

The VAWI–2 technique described above is especially suitable for the measurement of small optical path differences δ, say, smaller than 5λ. On the other hand, birefringent phase-plates, birefringent foils, and other extended plate-like double-refracting objects that produce higher optical path differences δ can effectively be tested by using the VAWI–3 technique. The latter is based on the same general principle as the former, but the distance d between the pointer lines L_1 and L_2 (Fig. 4) is reduced to the zero value. Consequently, a single pointer line is used. Initially, the zero-order interference fringe of the empty interference field is brought into coincidence with this line, light wavelength is then varied, and high-order fringes displaced by the object under study are consecutively brought into coincidence with the pointer line. The procedure leading to the final interferometric results is quite similar to that described above for the VAWI–2 technique. Since the distance d is now equal to zero, Eq. (13) takes the form of Eq. (10). If the term $B_{s1} D_{1s}$ is equal to unity or $B_{s1} D_{1s} \simeq 1$, we can also use Eq. (12) for calculating the initial interference order m_1.

5. Illustrating measurements

In order to illustrate the practical performance of the VAWI techniques described above, interferometric studies have been performed on some birefringent objects. Exemplary measurements of the spectral dispersion of fibre birefringence $B(\lambda)$ and of the dispersions $n_{\parallel}(\lambda)$ and $n_{\perp}(\lambda)$ of fibre refractive indices by using the VAWI–1 technique have been reported earlier [7]. Some other illustrating measurements given here refer to birefringent foils and phase retarders.

5.1. Cellophane foil

Table 2, Fig. 5, and Fig. 6 show the results of measurement of a cellophane sheet. Figure 5 follows from directly measured and visually observed parameters (b_s and q_s), while Fig. 6 represents graphically the results of a calculation process. It is worth while noting that a rough analysis of Fig. 5 indicates the wavelength λ_0 for which the tested cellophane foil manifests itself as an exact $\lambda/2$-plate. For this analysis it is sufficient to draw lines through the measurement points belonging to the m and $m+1$ interference orders as shown in Fig. 5 by dotted lines. Among these lines there is one which is nearly or even exactly horizontal; here there is a narrow spectral region which includes the wavelength λ_0. This particular wavelength is, in general, more precisely localized on the graph $\varrho(\lambda)$ as shown in Fig. 6; for λ_0 the relative retardation $\varrho = 0.5$. As can readily be seen, the dotted lines in Fig. 5 rise for $\varrho > 0.5$ and descend for $\varrho < 0.5$. The VAWI–2 technique offers the accuracy in determining λ_0 within ± 0.5 nm.

Table 2. Results of the measurement of a cellophane strip by using the VAWI–2 technique

q	$\Theta = +45°$; $m_1 = 10$				$\varrho = \delta/\lambda$
	b [μm]	λ [nm]	$m' = m_1 + q$	$\Delta' = m'\lambda$ [μm]	
0	229.55	661.0	10	6.6100	0.3956
−0.5	241.80	693.9	9.5	6.5921	0.3804
1	208.53	604.7	11	6.6517	0.4368
2	191.18	558.8	12	6.7056	0.4719
3	176.75	520.3	13	6.7639	0.5000
4	164.20	487.5	14	6.8250	0.5282
5	153.43	458.8	15	6.8820	0.5645
5.5	149.03	447.0	15.5	6.9285	0.5699
	$\Theta = -45°$; $m_1 = 11$				
	b [μm]	λ [nm]	$m'' = m_1 + q$	$\Delta'' = m''\lambda$ [μm]	
0	225.20	649.4	11	7.1434	0.4068
−0.5	236.13	678.6	10.5	7.1253	0.3885
1	206.63	599.6	12	7.1952	0.4463
2	190.43	556.7	13	7.2371	0.4734
3	176.75	520.3	14	7.2842	0.5000
4	165.15	489.5	15	7.3470	0.5332
5	154.88	462.7	16	7.4032	0.5621
5.5	149.98	449.7	16.5	7.4201	0.5670

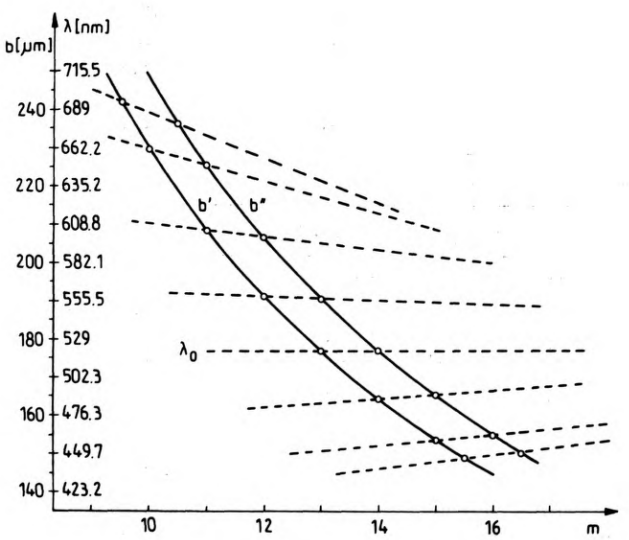

Fig. 5. Plots according to data listed in Table 2, columns 2 and 4

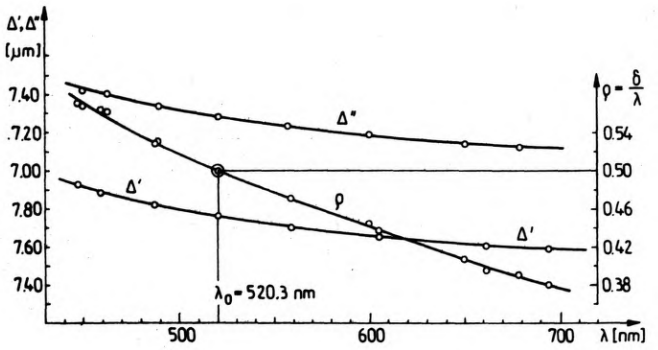

Fig. 6. Plots according to data listed in Table 2, columns 3, 5, and 6

5.2. Subtractive λ-plate

Table 3, Fig. 7, and Fig. 8 show the results of measurement of a subtractive λ-plate by using the VAWI–2 technique. The plate was made of quartz crystal and destined for a polarizing microscope. The subtractive birefringent phase plate consists of two crossed plates, one of which is polished to obtain a difference $t_2 - t_1$ in their thickness equal to δ/B, and the plates are then cemented together with their optical axes crossed.

The dotted lines in Fig. 7 are drawn through the measurement points for which

Table 3. Results of measurement of a quartz subtractive λ-plate by using the VAWI–2 technique

q	$\Theta = +45°$; $m_1 = 9$				$\varrho = \delta/\lambda$
	b [μm]	λ [nm]	$m' = m_1 + q$	$\Delta' = m'\lambda$ [μm]	
0	246.30	706.0	9	6.3540	0.7337
1	220.58	636.8	10	6.3680	0.8323
2	200.25	582.8	11	6.4108	0.9173
3	183.65	538.0	12	6.4560	1.0216
4	169.50	501.0	13	6.5130	1.1198
5	157.50	469.7	14	6.5758	1.1989
6	146.93	441.5	15	6.6225	1.3075
6.5	142.2	429.0	15.5	6.6495	1.3584
	$\Theta = -45°$; $m_1 = 11$				
	b [μm]	λ [nm]	$m'' = m_1 + q$	$\Delta'' = m''\lambda$ [μm]	
0	234.10	673.2	11	7.4052	0.7763
−0.5	245.48	703.8	10.5	7.3899	0.7345
1	214.70	621.0	12	7.4520	0.8639
2	197.38	575.1	13	7.4763	0.9227
3	184.08	539.7	14	7.5558	1.0226
4	172.20	508.2	15	7.6230	1.1049
5	161.65	480.5	16	7.6880	1.1842
6	152.03	455.0	17	7.7350	1.2473
7	143.94	433.5	18	7.8030	1.3414

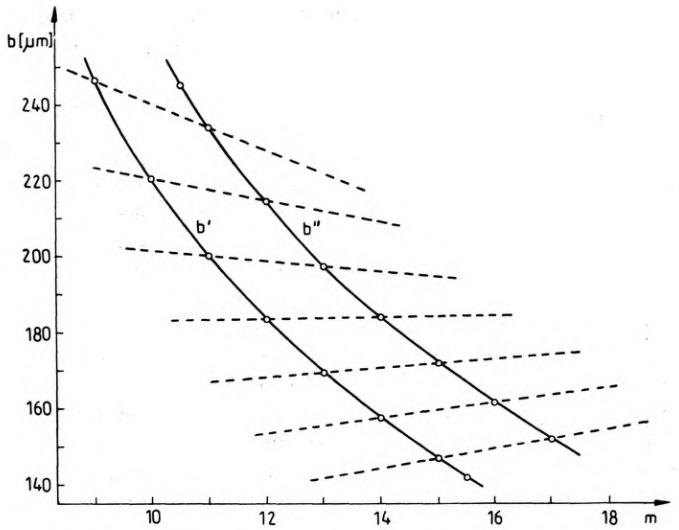

Fig. 7. Plots according to data listed in Table 3, columns 2 and 4

the interference order m differs by 2. As stated above (see Fig. 5), the line, that is nearly or exactly horizontal, indicates a narrow spectral region where there is the wavelength λ_0 for which the phase plate under study manifests itself as an exact, in this case, λ-plate. Originally, the tested plate was designed for $\lambda_0 \approx 556$ nm. The results of measurement listed in Table 3 and shown in Figs. 7 and 8 reveal that in fact $\lambda_0 = 538.9$ nm.

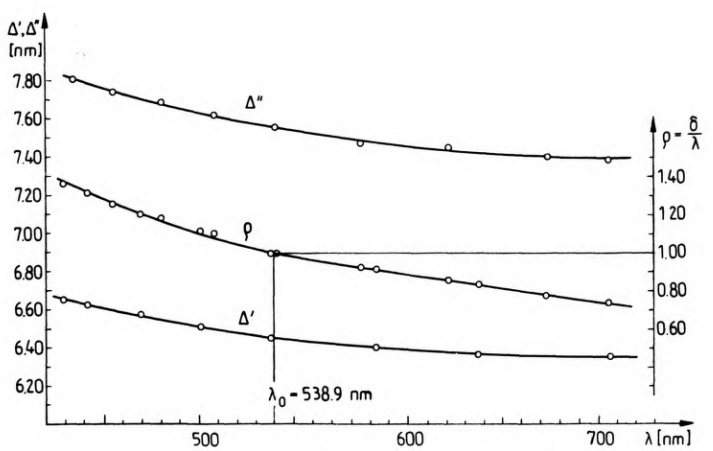

Fig. 8. Plots according to data listed in Table 3, columns 3, 5, and 6

5.3. High-order phase retarder

Birefringent retarders used in laser technology are frequently manufactured as high-order phase plates. Such a retarder, designed originally for a pulse ruby laser (emitting the wavelength $\lambda_R = 694.3$ nm) was tested by using the VAWI–3 tech-

Table 4. Results of the measurement of quartz high-order retarder by using the VAWI–3 technique

q	b [μm] for $\Theta = +45°$	b [μm] for $\Theta = -45°$	b [μm] mean value	λ [nm]	$m = m_1 + q$	$\delta = m\lambda$ [μm]	$B = n_e - n_o = \delta/653.412$ μm
0	226.90	228.40	227.65	655.90	$9 (= m_1)$	5.9031	0.009034
−0.5	239.79	242.79	241.29	692.48	8.5	5.8860	0.009008
0.5	214.33	216.56	215.45	623.29	9.5	5.9213	0.009062
1	203.90	205.40	204.65	595.50	10	5.9450	0.009098
1.5	194.20	195.68	194.94	568.60	10.5	5.9703	0.009137
2	184.92	187.10	186.01	545.10	11	5.9961	0.009177
2.5	177.08	179.32	178.20	524.00	11.5	6.0260	0.009222
3	170.05	171.63	170.84	504.40	12	6.0528	0.009263
3.5	163.22	164.48	163.85	486.37	12.5	6.0796	0.009304
4	156.85	157.87	157.36	469.50	13	6.1035	0.009341
4.5	151.20	152.10	151.65	454.13	13.5	6.1308	0.009383
5	145.48	147.02	146.25	440.25	14	6.1635	0.009433

nique. The results are listed in Table 4 and shown in Figs. 9 and 10. In contrast to the VAWI 2 technique, the plots b' and b'' are now symmetrical with respect to the zero interference order ($m = 0$) of the empty interference field. Consequently, the calculation procedure leading to the final results can be a simplified; first of all, the interfringe spacings b_1, b_2, b_3, ... measured for the azimuths $\Theta = +45°$ and $\Theta = -45°$ can be taken as the mean values (see the second, third, and fourth columns of Table 4), which serve then for reading the wavelengths λ_1, λ_2, λ_3, ... from the calibration plot $b(\lambda)$.

As can be seen, the tested quartz plate was the $(8+1/2)/\lambda$-retarder for $\lambda_0 = 692.48$ nm. The discrepancy between λ_0 and λ_R appeared to be small and tolerable in practice.

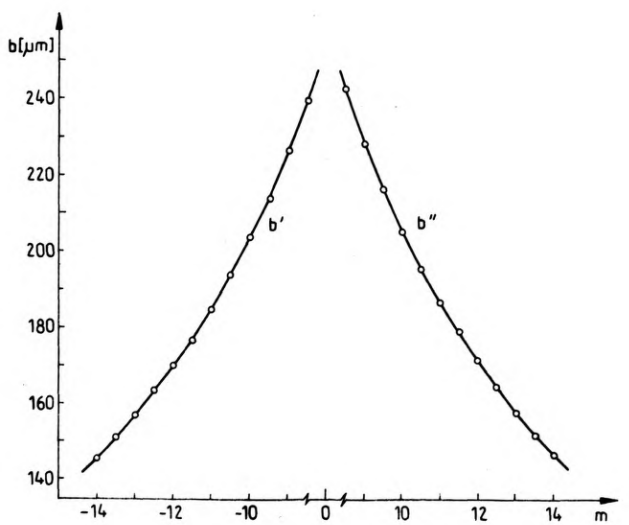

Fig. 9. Plots according to data listed in Table 4, columns 2, 3, and 6

This plate was also used for determining the birefringence dispersion $B(\lambda)$ of quartz crystal. In the literature we can find the refractive indices n_o and n_e, or their difference $n_e - n_o$, of quartz crystal for several spectral lines, e.g., D, e, C, and F, but different authors specify slightly different data (compare, e.g., [9] and [10]). The most unanimous value of quartz birefringence is specified for λ_D; it is equal to

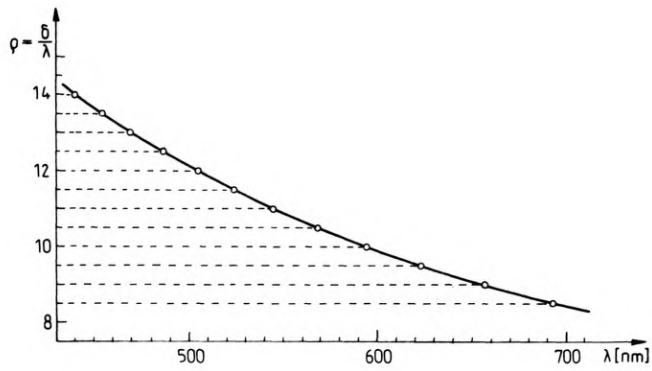

Fig. 10. Plot according to data listed in Table 4, columns 5 and 7

0.009109. This value has been inserted in the formula $\delta_D = B_D t$ and the optical path difference $\delta_D = \varrho_D \lambda_D = 10.10 \times 0.5893$ μm = 5.95193 μm has been read out from the plot $\varrho(\lambda)$ shown in Fig. 10. From these data it has resulted $t = 5.95193/0.009109 = 653.412$ μm. Assuming this value for t we get the quartz birefringences B listed in the last column of Table 4. Consequently the dispersion curve $B(\lambda)$ has been obtained (Fig. 11) from which the data listed in Table 5 has been read out.

Table 5. Birefringence dispersion of quartz crystal determined by using the VAWI-3 technique

Wavelength [nm]	Birefringence $n_e - n_o$	Wavelength [nm]	Birefringence $n_e - n_o$
440	0.009430	580	0.009122
450	0.009395	589.3 (D)	0.009109
460	0.009365	590	0.009108
470	0.009339	600	0.009094
480	0.009315	610	0.009081
486.1 (F)	0.009301	620	0.009068
490	0.009291	630	0.009056
500	0.009267	640	0.009045
510	0.009244	650	0.009035
520	0.009222	656.3 (C)	0.009030
530	0.009202	660	0.009025
540	0.009183	670	0.009016
546.1 (e)	0.009176	680	0.009008
550	0.009166	690	0.009000
560	0.009150	700	0.008992
570	0.009136		

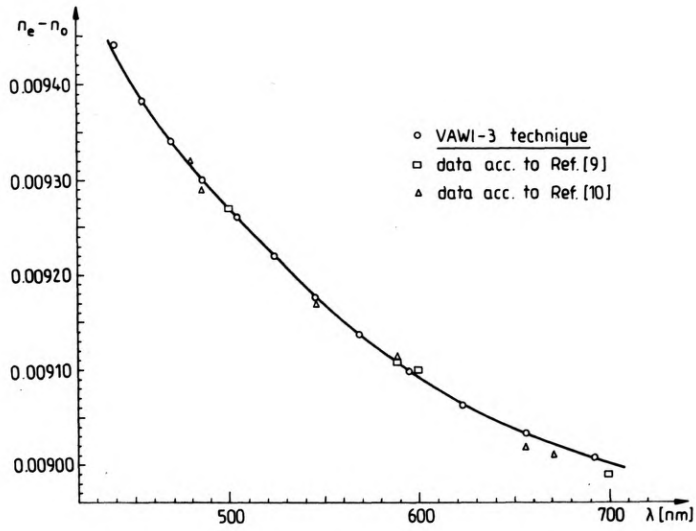

Fig. 11. Plot according to data listed in Table 4, columnes 5 and 8; birefringence dispersion of quartz crystal

6. Conclusions

The VAWI techniques offer a simple and accurate tool for examining birefringent objects, especially textile fibres, foils, phase plates, and the like objects. In comparison to the common interferometric techniques, which use monochromatic light of constant wavelength, the VAWI techniques presented here are more versatile and free from difficulties or oven possible errors in establishing the integral number of wavelength retardation when optical path differences δ to be measured are higher than λ.

When used to the microinterferometry of textile fibres, the VAWI techniques do not require a liquid immersion medium as is usual and a fibre under study may simply be surrounded by an air medium if the mean birefringence or mean refractive indices $n_{\parallel}$ and $n_{\perp}$ are determined [7].

When used for testing birefringent phase retarders (λ-, $\lambda/2$-, $\lambda/4$-plates) and other plate-like optical elements, the VAWI–2 or VAWI–3 technique permits us to determine the light wavelength λ_0, for which the retarder behaves as an exact λ-, $\lambda/2$- or $\lambda/4$-plate as accurately as 1 nm.

It is also worth while noting that the VAWI–2 and VAWI–3 techniques are suitable for fully automatic operation; it is selfevident that two pointer lines L_1 and L_2 (Fig. 4) or a single pointer line can be considered as slit apertures of photoelectronic detectors.

If the spectral dispersion of birefringence of a double-refracting interference system is similar to that of an abject to be examined, an interferometric method referred to as the object adapted variable wavelength interferometry (OAVAWI) is obtained, which enables the optical path differences (δ) to be measured very

accurately by using relatively simple means. Moreover, the OAVAWI method permits us to measure the object thickness. This quite specific method is covered by a separate paper [5].

References

[1] PLUTA M., Optica Applicata **15** (1985), 375–393.
[2] PLUTA M., Optica Applicata **16** (1986), 141–157.
[3] PLUTA M., Optica Applicata **16** (1986), 159–174.
[4] PLUTA M., Optica Applicata **16** (1986), 301–323.
[5] PLUTA M., Applied Optics (submitted for publication).
[6] DORAU K., PLUTA M., Przegląd Włókienniczy **35** (1981), 70–75, 128–133 (in Polish).
[7] PLUTA M., Przegląd Włókienniczy **39** (1985), 391–394 (in Polish).
[8] PLUTA M., Optica Applicata **12** (1982), 19–36.
[9] TOPORETZ A. S., *Monokhromatory*, (in Rusian), Gos. Izd. Tekh.-Teoret. Literatury, Moskva 1955.
[10] HARDY A. C. PERRIN F. H., *The Principls of Optics*, McGraw–Hill Book Company, New York–London 1932.

Received November 19, 1986

Интерферометрия с плавно-переменной длиной волны V. Применение для двоякопереломляющих предметов

Четыре предыдущих доклада, по теме интерферометрии с плавно-переменной длиной волны (VAWI) относятся к изотропическим предметам. В этой статье дан оригинальный метод VAWI для проходящего света и его видоизменения, методы VAWI–2 и VAWI–3 применены для анизотропических предметов таких как: текстильные волокна, фазовые пластинки (ретардеры), фольги и другие тому подобные предметы.